European Polymer Journal 117 (2019) 77–85

Contents lists available at ScienceDirect

European Polymer Journal

journal homepage: www.elsevier.com/locate/europolj

Fabrication of epoxy modified polysiloxane with enhanced mechanical properties for marine antifouling application

Xun Sun[a,b], Rongrong Chen[a,b,c,*], Xiang Gao[b], Qi Liu[a,c], Jingyuan Liu[a], Hongsen Zhang[a], Jing Yu[a], Peili Liu[b,d], Kazunobu Takahashi[b], Jun Wang[a,b,*]

[a] Key Laboratory of Superlight Material and Surface Technology, Ministry of Education, Harbin Engineering University, 150001, China
[b] Institute of Advanced Marine Materials, College of Materials Science and Chemical Engineering, Harbin Engineering University, Harbin 150001, China
[c] HIT (Hainan) Military-Civilian Integration Innovation Research Institute Co., Ltd., Hainan 572427, China
[d] Qingdao Advanced Marine Material Technology Co., Ltd, Qingdao 266100, China

ARTICLE INFO

Keywords:
Epoxy
Polysiloxane-based coating
Mechanical properties
Antifouling

ABSTRACT

Marine biofouling is a catastrophic problem for maritime industries, which catches researchers' attention. Antifouling coatings have been proved to be an effective approach to against fouling organisms. Herein, we firstly synthesized polydimethylsiloxane with aminopropyl-terminated pendant groups (APDMS) through a ring opening polycondensation, and then APDMS was reacted with bisphenol A type epoxy resin (DGEBA) to form the epoxy modified polysiloxane-based resin (EAPDMS). The curing behavior of DGEBA/APDMS was studied by differential scanning calorimetry (DSC) with a non-isothermal curing method. The adhesion strength of EAPDMS was remarkably improved. The results of dynamic mechanical properties (DMA) and tensile tests showed an obvious enhancement of mechanical properties in the modified resin system. Marine field tests revealed that coatings exhibited excellent antifouling performance within 3 months. In brief, the EAPDMS coatings possess outstanding mechanical properties and excellent adhesion strength, showing high potential in the marine antifouling field.

1. Introduction

In the realm of maritime industries, marine biofouling has been known to be a catastrophic problem, leading to detrimental results, including acceleration of biocorrosion, increasing hydrodynamic drag, fuel consumption and the transportation of invasive species, which have negative effects on human activities in the ocean [1,2]. Marine biofouling, generally known as an undesirable settlement and accumulation of microorganisms, algae and animals occurred on objects, especially man-made structures submerged in seawater [3,4]. Among all the solutions for combating marine biofouling, the self-polishing coating system containing tributyltin (TBT) was proved to be the most effective method. Unfortunately, they have been banned all across the world since 2008 because of their persistent toxicity to resident marine organisms [5]. Nowadays, many efforts have been made to develop eco-friendly and effective antifouling materials to satisfy the need for hindering and regulating marine biofouling. For instance, slippery liquid-infused surfaces [6,7], functional polymers involving self-polishing copolymers [8,9], fouling release polymers [10,11], zwitterionic polymers [12,13], and protein resistant polymers [14,15] have been investigated for this purpose. Among the materials mentioned above, polysiloxane-based (PDMS-based) material is the most promising candidate for marine antifouling applications. Particularly, the polysiloxane can lower the adhesion strength between the fouling organisms and the coating because of its low surface energy (~22 mN m^{-1}) and low modulus [15,16], which make the organisms easy to be removed. However, the non-stick property and highly rotatable Si-O backbone of polysiloxane tend to lower adhesion strength between the coatings and substrates [17], which lead to peel-off and vulnerability of the coatings during their service life.

To improve the mechanical properties and adhesion strength of polysiloxane-based materials, chemical approaches such as introducing diisocyanates [18–21] and epoxy resin [22–25] into the polymer matrix have been employed to modified PDMS. Considering the large disparity of the solubility parameter between polyurethane (PU) and PDMS, scientists tried to synthesize PU modified PDMS materials to meet the requirements of mechanical properties [18–21]. Chao Liu et al [18] reported a series of polydimethylsiloxane-based polyurea that exhibit a larger tensile strength (about 14 MPa) and strain capability than that of PDMS. The PDMS-PU coatings showed an adhesion strength above

* Corresponding authors at: Key Laboratory of Superlight Material and Surface Technology, Ministry of Education, Harbin Engineering University, 150001, China.
E-mail addresses: chenrongrong95@163.com (R. Chen), zhqw@sohu.com (J. Wang).

https://doi.org/10.1016/j.eurpolymj.2019.05.002
Received 27 January 2019; Received in revised form 19 April 2019; Accepted 3 May 2019
Available online 03 May 2019
0014-3057/

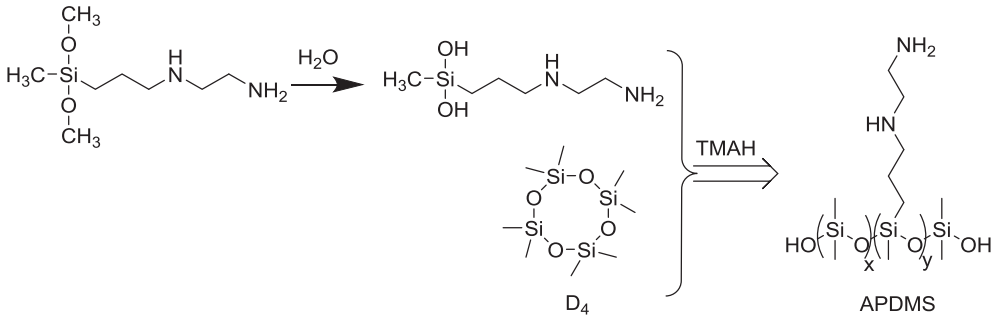

Scheme 1. Synthesis diagram of APDMS.

1.0 MPa. Xinxiu Wu et al [20] developed a series of PDMS-PU elastomers that possessed the elongation at break from 876% to 1204%, while the tensile strength was from 2.33 to 3.06 MPa. Nevertheless, PU is sensitive to hydrolytic degradation. The instability of PU has limited their long-term application. Furthermore, the Si—O—C bond that formed by the reaction between Si—OH and NCO group is easy to hydrolyze [26,27], leading to the poor hydrolytic stability. The phase separation between PU and PDMS also weaken the internal forces of the polymer and have the opposite effect [26]. The disadvantages mentioned above limit their applications in the marine environment.

Epoxy resins, owing to its remarkable mechanical properties, chemical resistance, bonding strength and electrical insulation, have been widely used in the paint industry. When the epoxy is blended into polysiloxane matrix, evident enhancement of mechanical and adhesion properties was observed [24,28–30], which can be attributed to more rigid molecular chain structures, higher crosslinking density and polarity groups' interaction. However, a large disparity of the solubility parameter between epoxy resin (10.9) and polysiloxane (7.4–7.8) made them easy to form a phase-separated structure [25,31] which affected the resin's performance. Similarly, the high surface energy of epoxy resins cannot meet the fouling release requirements. To improve the compatibility between epoxy and polysiloxane, scientists have synthesized polysiloxane-based functional polymers with active hydrogen groups or epoxide groups across-linkers [32]. Rath et al [25] reported a two-component silicone modified epoxy foul release coatings can efficiently remove macrofouling, mechanical measurements show that the coatings possess lower tensile strength and higher elongation.

In this work, we designed an epoxy modified polysiloxane coating. A series of polysiloxane copolymers with aminopropyl-terminated pendant groups were synthesized via a ring-opening polycondensation of octamethylcyclotetrasiloxane and 3-(2-aminoethylamino) propyl-dimethoxymethylsilane, followed by the introduction of bisphenol A type epoxy resin (DGEBA) into the polysiloxane copolymers, forming a ladder-like structure. DSC (Differential Scanning Calorimetry) in a non-isothermal curing method was applied to study the curing behaviors of DGEBA/APDMS. DMA (Dynamic Mechanical Properties), tensile test, and adhesion test were carried out to evaluate mechanical properties and the adhesion strength of the modified system. SEM (Scanning Electron Microscope), CA (Contact Angle), and SFE (Surface Free Energy) were performed to evaluate the fracture surfaces and surface properties of EAPDMS. Laboratory assay was conducted with Diatom Nitzschia closterium to check coatings' antifouling performance. The antifouling performance was also checked by marine field test in the Yellow Sea, China. Our goal is to exploit high-performance antifouling systems with remarkable mechanical properties.

2. Experimental section

2.1. Materials

Octamethylcyclotetrasiloxane (D_4, Industrial grade, 98%) was purchased from Wuhan Xinyu Chemical Co. Ltd.. 3-(2-aminoethylamino) propyl-dimethoxymethylsilane (AEAPDMS) was purchased from Aladdin. Tetramethylammonium hydroxide pentahydrate (TMAH) was purchased from Xiya Reagent. Bisphenol A type epoxy resin (E51, DGEBA, epoxy equivalent weight: 0.51 mol/100 g) was purchased from South Asia electronic materials (Kunshan) Co. Ltd.. Jeffamine® T403 polyetheramine was purchased from Huntsman. Sylgard 184 PDMS elastomer was purchased from Dow Corning Corporation. SILIKOPON EF was purchased from Evonik. All the reagents were used as received without further purification. Deionized water was purified using a Milli-Q Plus system (Millipore, Schwalbach, Germany).

2.2. Synthesis of polysiloxane with aminopropyl-terminated pendant groups

The polymer was synthesized in accordance with previous literatures [33–35] with some modification via a procedure illustrated in Scheme 1. Typically, AEAPDMS, D_4, a water solution of TMAH (25 wt %, 0.1 ml) were charged into a four-necked round-bottom flask equipped with a tetrafluoroethylene stirrer, a thermometer, a condenser with vacuum-pumping system, and nitrogen protection device. The mixture was heated to 95 °C and kept for 40 min to finish a hydrolysis reaction of AEAPDMS. Then the polymer was synthesized via polycondensation by mixing D_4 and hydrolysis product of AEAPDMS at 110 °C. The reaction was carried out for another 2 h after the mixture undergoes "transparent-turbid-transparent" procedures under vacuum distillation (< 1 kPa). TMAH (25 wt%, 1 ml) was added into the mixture as blocking agent to accomplish the polymerization in 4 h at 125 °C with nitrogen protection. The system was quickly heated to 155 °C and kept for 0.5 h to remove the excessive TMAH. At last, the mixture was purified by vacuum pumping process to remove the unreacted or rebuilt cyclic oligosiloxanes. The colorless and viscous polymer was denoted as APDMS-x (x = 1, 2, 3, 4, or 5). The chemical structures of synthesized polymers were confirmed by Proton Nuclear Magnetic Resonance Spectroscopy and Fourier Transform Infrared Spectroscopy, respectively. The hydrochloric acid/ethyl alcohol method was applied to determine the amine value of the as-synthesized polysiloxanes with aminopropyl-terminated pendant groups.

2.3. Amine value and percentage of amine segments in APDMS

The measurement of the amine value of APDMS [33,35] polymers was based on the reaction mechanism of hydrochloric acid and amine groups, which is shown in Scheme 2. The experiments were performed three times for each sample. 2% ethanol solution of APDMS with bromophenol blue as an indicator was titrated with 1 mol/L hydrochloric acid. The amine value was decided by equation (1) as followed:

$$RNH_2 + HCl \rightarrow RNH_3^+Cl^-$$

$$R_2NH + HCl \rightarrow R_2NH_2^+Cl^-$$

Scheme 2. The reaction mechanism of hydrochloric acid and amine groups.

$$P = [C_{HCl}\cdot(V^1_{HCl}/M_1 + V^2_{HCl}/M_2 + V^3_{HCl}/M_3)]/3 \quad (1)$$

where P is the amine value of APDMS, V^1_{HCl}, V^2_{HCl}, V^3_{HCl} are the volume of hydrochloric acid consumed during the titration, M_1, M_2, M_3 are the mass of APDMS weighted each analysis, and C_{HCl} is the concentration.

The percentage of amine segment in APDMS was calculated by following equations as:

$$Q = X/(X + Y) \quad (2a)$$

$$X = P/2 \quad (2b)$$

$$Y = [(1 - X\cdot 160 \times 10^{-3})/74] \times 10^3 \quad (2c)$$

where Q and P represent the percentage of amine segments in APDMS and amine value of APDMS, Y represents the mol of dimethyl siloxane segments in 1 g APDMS, X represents the mol of amine segments in 1 g APDMS. The molar mass of the amine segment and dimethyl siloxane segments are 160 g/mol and 74 g/mol, respectively.

2.4. Curing of epoxy modified polysiloxane resins

The epoxymodified silicone resin was prepared by blending a stoichiometric amount of APDMS and DGEBA. The equivalent ratio between the epoxy resin and APDMS was decided by the epoxide equivalent of DGEBA and the amine value of APDMS. The well-blended mixtures were degassed to remove air bubbles in a vacuum oven. For the adhesion test and marine filed test, the mixtures were brushed on glass fiber reinforced epoxy resin plates. For DMA test and tensile test, the mixtures were poured into a stainless steel mold. The specimens were transferred into a convection oven which was preheated to 80 °C and cured for 4 h and 120 °C for another 2 h. The samples with different epoxy content were denoted as EAPDMS-x (x = 1, 2, 3, 4, or 5). The blank sample was prepared by blending a stoichiometric amount of T403 and DGEBA (mass ratio:4:10).

2.5. Characterization methods

The proton nuclear magnetic resonance spectroscopy (^{1}H NMR) spectrum was recorded on a Bruker Advance III-400 spectrometer (400 MHz) with $CDCl_3$ as the solvent. A fourier transform infrared spectroscopy (FTIR) spectrum was obtained by using potassium bromide disks with a Perkin Elmer Spectrum 100 Fourier transform infrared spectrometer to confirm the chemical structures of APDMS, EAPDMS and E51. The scanning range was from 400 cm^{-1} to 4000 cm^{-1} and the spectral resolution was set to 4 cm^{-1}. To understand the non-isothermal curing behavior of the DGEBA/APDMS system, isothermal differential scanning calorimeter (DSC, TA Instruments, Q2000) tests were conducted in nitrogen atmosphere (20 ml/min) with a heat rate of 3, 4.5, 7, 10 and 10 °C /min from 30 °C to 200 °C. The epoxy modified polysiloxane samples were prepared by cryogenically fracture method in liquid nitrogen. The fracture surface was coated with gold. A JEOL JSM-6480A microscope was used to take the images at an accelerating voltage of 5 kV. The coatings' pull-off strength was estimated by an automatic adhesion tester (PosiTest AT-A) in accordance with ASTM D4541-09 on the glass fiber reinforced epoxy resin panel with a measurement area of 20 mm in diameter and the pull rate of 0.2 MPa/s. An average value of five different points was calculated on each sample. The coatings' surface contact angle was measured by a Contact Angle System OCA50 (Dataphysics) at room temperature. An average value was calculated from five different points on each point. Water and N, N-dimethylformamide liquid were used in this experiment to obtain data for calculating the surface energy. The mechanical properties of epoxy modified polysiloxane resins were studied by Dynamic Mechanical Analysis measurements (DMA, TA Instruments, Q800) and tensile tests (Instron model 3365 tensile tester). The samples for DMA test (50 mm long, 30 mm wide, and 2 mm thick) were analyzed from −130 °C to 60 °C at a frequency of 1 Hz. The tensile test was performed at a rate of 1 mm/min with a strip-type sample (80 mm long, 30 mm wide, and 30 mm thick) at room temperature. An average value of five different points was calculated on each sample.

2.6. Theoretical bases of DGEBA/APDMS's curing reaction kinetics

Generally, the reaction degree and reaction rate of a curing reaction can be investigated by the thermal data acquired from DSC tests. The correlated data is assumed by equations [36–38] as follows:

$$\alpha = \int_0^t dHdt/\Delta H \quad (3a)$$

$$d\alpha/dt = (dH/dt)/\Delta H = k(T)f(\alpha) \quad (3b)$$

where H, t, ΔH and α represent the DSC heat flow, the reaction time, the overall reaction exothermal value and the conversion, respectively. K (T) is the reaction rate constant in relation with the temperature and follows the Arrhenius law (Eq. (4)).

$$k(T) = A\exp(-E_a/RT) \quad (4)$$

where A, E_a, T represent the frequency factor, the activation energy and the temperature, respectively. R is the universal gas constant (8.314 J mol^{-1} K^{-1}).

2.7. Laboratory assay

Diatom adhesion experiments. Diatom *Nitzschia closterium* (*N. closterium*) was obtained from Xiamen University. EAPDMS samples were placed in Erlenmeyer flasks and immersed into diatom suspensions. After 24 h (12 h/12 h light-dark) immersing at 23 ± 2 °C, samples were washed with filter-sterilized seawater to remove unattached diatoms. The samples are examined with a fluorescence microscope (Nikon ECLIPSE Ci-L). Ten random fields (20× magnification, 0.916 mm^2/per field). of view were recorded for each sample. The *N. closterium* settlement results were analyzed with One-Way ANOVA, followed by a Tukey post-test.

Diatom activity experiments. The Diatom suspension and the algal nutrient solution are mixed (1/50, v/v) and put into Erlenmeyer flasks with test samples at 23 ± 2 °C for 15 days (with a 12 h/12 h light-dark cycle). The diatom count was determined with a hemocytometer and recorded every day.

2.8. Marine antifouling field studies

Epoxy modified silicone coatings were coated on the panels (300 × 150 × 3 mm^3) and arranged at a depth of 1 m in the Yellow Sea (37°09′N, 122°32′E) from September 2017 to June 2018 to evaluate their antifouling performance. The test panels were raised from the sea and photographed before and after a lightly wash. An epoxy resin (E51) coated panel, two polysiloxane resin (Sylgard 184, Dow Corning and SILIKOPON EF, Evonik) coated panels were chosen as control panels.

3. Result and discussion

3.1. Characterization of APDMS and EAPDMS

Fig. 1 shows the ^{1}H NMR spectrum (a) of APDMS-1, FT-IR spectra of APDMS-1 (b) and E51, APDMS-1 and EAPDMS-1 (c). The formulation of APDMS is listed in Table 1. The molecular structure of the synthetic copolymer was confirmed by ^{1}H NMR (Fig. 1a). Peaks of active hydrogen in the spectra are not obvious since various active hydrogen (−NH−, $-NH_2$ and −Si−OH) in the polymer can make a rapid exchange reaction [36]. In this case, the appearance of coupling and division between active hydrogen and the hydrogen in the adjacent group cannot be observed, resulting in only one active hydrogen single peak. To verify the existence of various active hydrogens, FTIR spectrum of

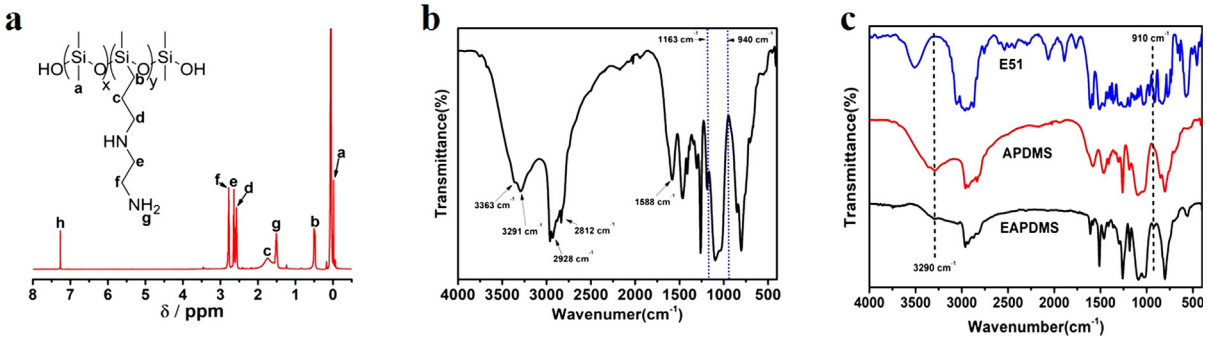

Fig. 1. ^{1}H NMR spectrum (a) of APDMS-1, FT-IR spectra of APDMS-1 (b) and E51, APDMS-1 and EAPDMS-1 (c).

Table 1
Formulation of the as-synthesized polysiloxanes with aminopropyl-terminated pendant groups.

Sample name	D_4 (ml)	AEAPDMS (ml)	Amine Value (mmol/g)	Percentage of Amine segments (%)
APDMS-1	100	125	5.23	24.4
APDMS-2	100	175	6.92	36.6
APDMS-3	100	200	7.05	37.5
APDMS-4	100	400	8.63	50.9
APDMS-5	100	900	9.23	56.8

Table 2
Formulations of epoxy modified polysiloxane resins.

Sample name	APDMS (mmol)	DGEBA (mmol)
EAPDMS-1	52.3	26.2
EAPDMS-2	69.2	34.6
EAPDMS-3	70.5	35.2
EAPDMS-4	86.3	43.1
EAPDMS-5	92.3	46.2

APDMS-1 (Fig. 1b) was recorded. The broad peaks at 3363 cm^{-1}, 3291 cm^{-1} are ascribed to blended vibrations of N—H bonds in primary amino's antisymmetrical and symmetrical vibration, secondary amino's stretching vibration and O—H bonds in silanol groups. The peak at 1588 cm^{-1} is attributed to the N—H bond's in-plane deformation vibration of secondary amino in pendant groups. The active hydrogen of amine on the pendant group of APDMS could react with the epoxy group to form a ladder-like structure. The formulation of epoxy modified polysiloxane resins is shown in Table 2. The epoxy group ring-opening reaction was confirmed by FTIR in Fig. 1c. For epoxy modified polysiloxane resin EAPDMS, peak intensities in 3290 cm^{-1} and 910 cm^{-1} significantly decreased, indicating the formation of cross-linked epoxy-silicone network.

3.2. Non-isothermal curing reaction

Fig. 2 shows the non-isothermal curing behavior of DGEBA/APDMS-3 at various heating rates carried out by DSC tests. In Fig. 2, for each DSC curve, an evident single exothermic peak was observed. The higher the heating rate was, the higher temperature range and broader peak was achieved. A similar trend can be acquired about Onset reaction temperatures (T_{onset}), peak temperatures (T_{peak}) and end temperatures (T_{end}), as shown in Table 2. It can be concluded that heating rate has little effect on the reaction enthalpy, which were between 264.4 J/g and 282.8 J/g, as shown in Table 3. T_{peak} of DGEBA/APDMS-3 system is about 10 °C lower than that of other silicon-amine curing agents at the same heating rate (4.5 °C /min) [39], which could be attributed to the high chain flexibility of synthetic APDMS, indicating APDMS's high reactivity.

Fig. 2b and c show the conversional curves of DGEBA/APDMS-3 by applying Eq. (3a). Evidently, there are three sections can be obtained based on the curve variation tendencies in Fig. 2b. At the initial stage of curing ($\alpha \leq 10\%$), the reaction rate α increased slowly. Whereafter, α increased much faster at the middle stage ($10\% \leq \alpha \leq 90\%$) and ended with a plateau ($\alpha \geq 90\%$). From the middle stage of the curing procedure, α rised steeply with the increase of heating rate, which is attributed to active functional groups' violent reaction and acceleration of the exothermic reaction. Fig. 2c shows the reaction rate dα/dt grows equably with the heating rate and the peak reaction rate (αp) presents within the conversion scope of 0.605–0.609. As a result, it can be concluded that the curing kinetics of DGEBA/APDMS are influenced by the heating rate, which hardly affects the fundamental of curing reaction.

3.3. DMA tests

Fig. 3a shows the curves of loss factor as a function of temperature to show the intermolecular interaction information of EAPDMS by DMA tests. The glass transition temperature (T_g) of the modified polysiloxane resin first increased and then decrease with epoxy content, reaching the highest value at EAPDMS-3 (see Table 4). In the beginning, the increasing T_g of the modified resin is ascribed to the high crosslinking density, which restricts polymeric segmental movement in EAPDMS. The following decrease in T_g is ascribed to insufficient crosslinking due to steric hindrance and uncured epoxy. It can be further verified by FTIR (Fig. 1b) as the peak intensity in 910 cm^{-1} reached the minimum at EAPDMS-3 and then increased.

Fig. 3b shows the storage modulus of EAPDMS at 25 °C. The storage modulus showed a similar trend as T_g, which reached a maximum value at EAPDMS-3 (78.82 MPa). Because of the rigid phenyl groups from epoxy segments and high crosslinking density, the storage modulus of EAPDMS is much larger than commercially available silicone Sylgard 184.

3.4. Mechanical properties

Table 5 lists the data obtained from tensile tests to examine the mechanical properties of EAPDMS. Generally, the epoxy modified polysiloxane resins showed higher tensile strength, modulus and lower elongation at break than that of pure silicone resin. As shown in Table 5, a significant improvement of tensile strength was obtained from EAPDMS-1 to EAPDMS-3. When the content of epoxy increased, the modified system could withstand more stress due to the rigid structure in the epoxy chain. The following decreased tensile strength with epoxy content is ascribed to the lower cross-linking density of the modified system and the lower strength of APDMS molecular chain. The variation of elongation at break and modulus are similar as the variation of tensile strength. The breaking elongation of the EAPDMS resin increased almost two times to 92% from EAPDM-1 to EAPDMS-3. When the epoxy content increased persistently, the breaking elongation

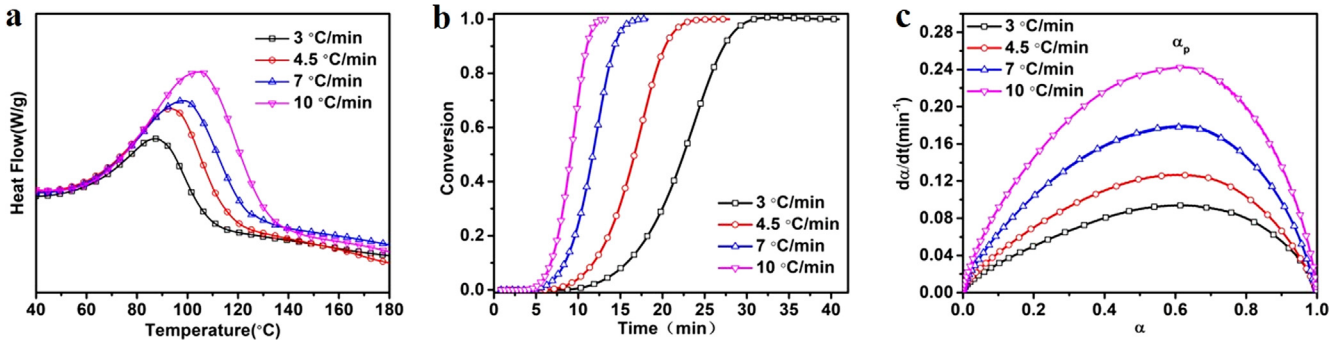

Fig. 2. Non-isothermal thermographs (a), conversion degree as a function of temperature (b), reaction rate dα/dt as a function of conversion (c) of DGEBA/APDMS-3.

Table 3
Typical parameters for characterizing the curing reaction of DGEBA/APDMS-3 under various heating rates.

β (°C/min)	T_{onset} (°C)	T_{peak} (°C)	T_{end} (°C)	ΔH (J/g)
3	43.6	88.16	125.0	270.6
4.5	46.7	94.04	134.7	282.8
7	49.8	99.17	140.8	266.2
10	52.2	105.71	150.9	264.4

Table 4
Dynamic mechanical analysis date of EAPDMS-x.

Sample name	T_g (°C)	tan δ
EAPDMS-1	29.4	0.30
EAPDMS-2	42.0	0.52
EAPDMS-3	49.1	0.41
EAPDMS-4	41.6	0.39
EAPDMS-5	40.3	0.36

sharply declined because of the poor cross-linking density and the weak interface boundaries between the siloxane and the unreacted epoxy resin [40,41]. The decrease of toughness in modified resins is ascribed to the presence of flexible siloxane linkages, free rotation of the Si—O—Si bonds and weak interaction between the siloxane and the unreacted epoxy resin lead to the decrease of toughness in modified resins [42].

3.5. The adhesion strength of EAPDMS coatings

Fig. 4 shows the EAPDMS-x coatings' adhesion strength on glass fiber reinforced epoxy resin panels. The Silicone 184 exhibits a low adhesion strength of ~0.4 MPa while the adhesion strength of modified polysiloxane coatings showed a much higher adhesion strength, which increases with the epoxy content. As the epoxy content increased in the modified coating system, more hydroxyl groups were generated from the epoxide ring-open reaction, contributing to the adhesion strength. In addition, the crosslinking density decreased in EAPDMS-4 and EAPDMS-5, providing more polarity groups in the coating system. Therefore, the coatings' adhesion strength increased with epoxy content [43].

Table 5
Mechanical properties of the epoxy modified silicone samples.

Sample name	Tensile strength (MPa)	Elongation at break (%)	Modulus (MPa)	Toughness (J/M^3)
EAPDMS-1	22.9 ± 2.5	60 ± 5	116.5 ± 0.1	11.1 ± 0.7
EAPDMS-2	28.8 ± 0.5	72 ± 4	285.0 ± 0.6	9.7 ± 0.4
EAPDMS-3	28.5 ± 0.9	92 ± 7	303.4 ± 0.4	7.6 ± 0.1
EAPDMS-4	3.7 ± 0.7	41 ± 6	14.8 ± 0.5	0.8 ± 0.6
EAPDMS-5	3.5 ± 1.0	47 ± 4	9.7 ± 0.4	0.8 ± 0.4
Silicone 184	2.8 ± 1.9	237 ± 3	1.1 ± 0.1	2.1 ± 0.3

3.6. Fracture morphology analysis

Fig. 5 shows the SEM of fracture surfaces of EAPDMS. In Fig. 5a–c, the miscibility between DGEBA and APDMS is enhanced, due to a higher amount of epoxide groups participate into the crosslinking reaction with the increasing of epoxy content. This morphology was consistent with that observed using SEM with EDS spectra and elemental mappings as shown in Fig. S2. The uniformly distributed silicon indicated that polysiloxane segments are well distributed in the modified resin system. Fig. 5d and e shows completely different signs with a brittle-fracture morphology because of the reduction of cross-linked

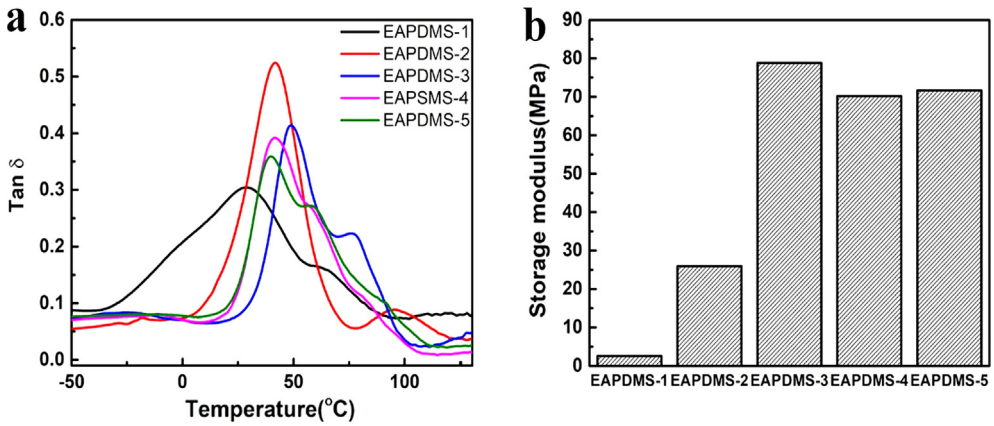

Fig. 3. Tan delta versus temperature (a), and Storage modulus (25 °C) (b) of EAPDMS.

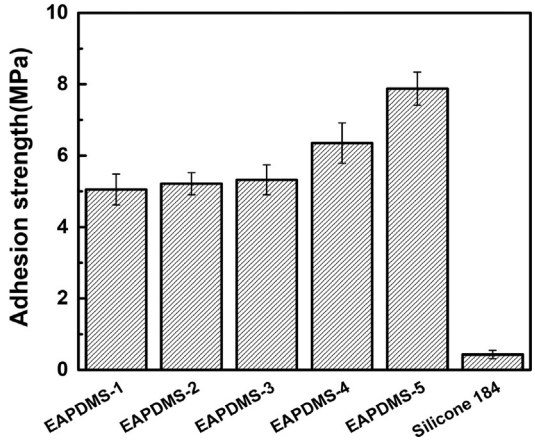

Fig. 4. The EAPDMS-x's adhesion strength to the substrate.

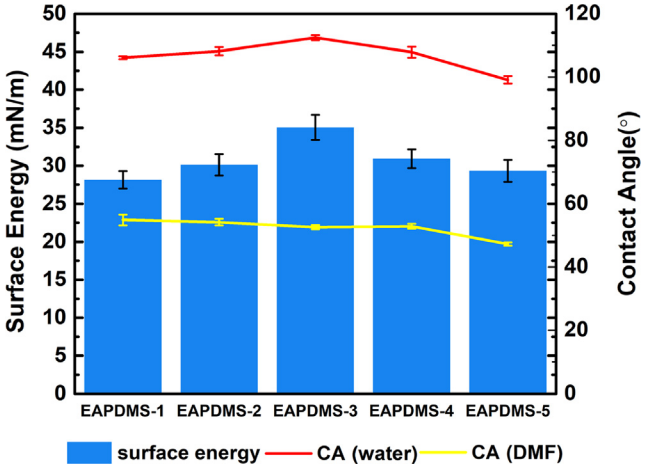

Fig. 6. Surface energy, CA (water) and CA (DMF) of the EAPDMS.

density in the epoxy modified polysiloxane matrices and the weak interface boundaries between the siloxane and the unreacted epoxy resin attributed to the unreacted DGEBA [41,44].

3.7. Surface properties

Fig. 6 shows the surface energy and the CA (water, DMF) of the EAPDMS. After DGEBA was incorporated, the surface energy increased and EAPDMS-3 achieved the highest value, which was ascribed to the growing amount of polar groups created by the inner cross-linking reaction [43,44]. The CA (DMF) of the modified coatings showed few fluctuation, and the CA (water) of the modified coatings were all above 90°, indicating hydrophobic nature arising from polysiloxane segments.

3.8. Laboratory assay

Fig. 7a–f shows the fluorescent microscope images of Silicone 184 as control and EAPDMS coatings. Evidently, a large number of *N. closterium* clung to the surface of control sample. Fig. 7g shows the Growth curves of *N. closterium* populations exposed to EAPDMS. Compared with the PDMS coating, the EAPDMS coatings significantly inhibited the growth of *N. closterium* populations. As illustrated in Fig. 7h, about 80% amount of *N. closterium* decreased on EAPDMS coatings in contrast with the control sample. The attached diatom density differences among the EAPDMS coatings were not significant (One-Way ANOVA, $p > 0.05$. Fig. 7h) [45,46]. In accordance with the zeta potential of EAPDMS coatings at pH = 8.0 (Fig. S4), with the crosslinking density increasing, EAPDMS-3 possessed the peak value of the zeta potential (+33.56 mV) due to the cation structure of primary amine and secondary amine from APDMS pendant groups. This EAPDMS coatings impressive effect of anti-diatom performance may be correlated with the cation structure of EAPDMS [47] and the fouling release performance [1,48–50] of PDMS. We hypothesise that the cation structure helped to maximize anti-diatom performance [47,51–54].

3.9. Field tests

Fig. 8 shows photographs of EAPDMS-x, Evonik EF, Silicone 184 and pure epoxy resin coated panels after immersing in the Yellow Sea, China. After 30 days' immersion, the epoxy coated panel was covered by fouling organisms involving barnacles, sponges and algae, demonstrating a serious fouling situation in the field test site. The panels coated with commercially available silicone resins (Silicone 184 and Evonik EF) had hard fouling organisms after 30 days immersion and the organisms grew up slowly after 90 days immersion. In contrast, the panels coated with EAPDMS-x were barely fouled by organisms. With 90 days immersion, the EAPDMS coating surfaces were still clean. The EAPDMS-5 sample surface was slightly fouled by slime. After 270 days of field test, the control samples were polluted seriously by marine

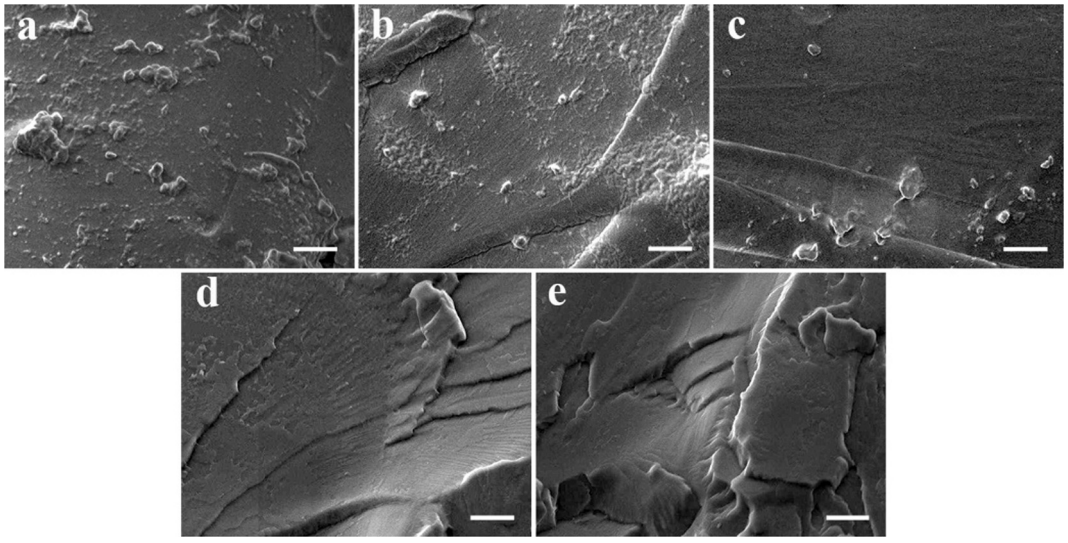

Fig. 5. SEM images of EAPDMS-1 (a), EAPDMS-2 (b), EAPDMS-3 (c), EAPDMS-4 (d), EAPDMS-5 (e).

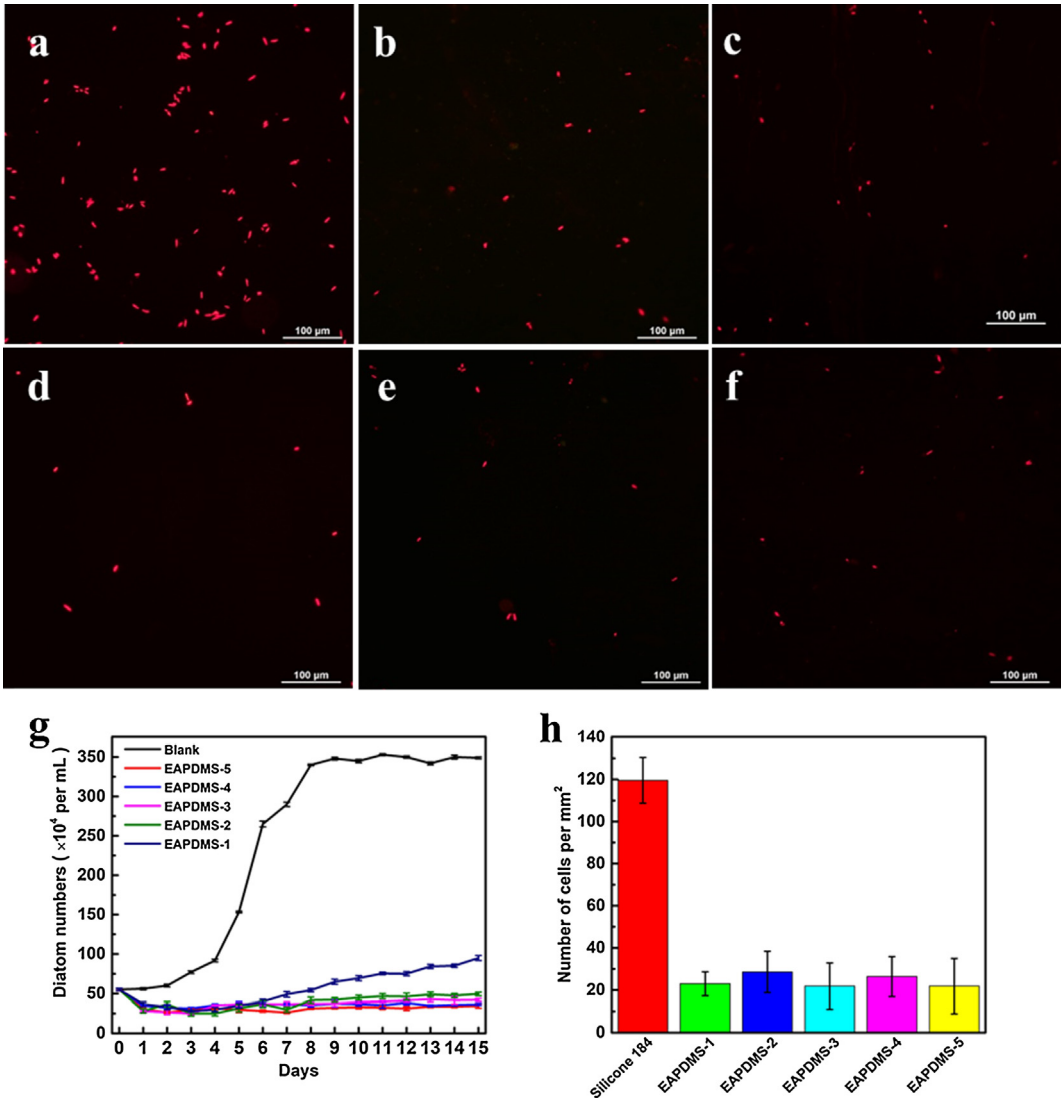

Fig. 7. The representative fluorescent microscope images of N. closterium on (a) Silicone 184, (b) EAPDMS-1, (c) EAPDMS-2, (d) EAPDMS-3, (e) EAPDMS-4, and (f) EAPDMS-5, the Growth curves of N. closterium populations exposed to EAPDMS (g) and N. closterium settlement on the EAPDMS coatings (h). Error bars correspond to standard deviations.

organisms. The EAPDMS coatings were covered by slime films. Evidently, their fouling extent was less than that of the control samples. This may be caused by the coupled effect of the low surface energy and the positive surface charges. The EAPDMS-3 sample shows excellent fouling release ability. The coating surface of EAPDMS-1, EAPDMS-4 and EAPDMS-5 are visibly covered by the slime fouling due to the poor anti-slime ability of polysiloxane elastomer.

4. Conclusions

In conclusion, we have synthesized APDMS via a ring-opening polycondensation of D_4 and AEAPDMS. The synthetic APDMS exhibited a high reactivity than other silicon-amine curing agents. Through the incorporation of DGEBA, novel epoxy modified polysiloxanes with a ladder-like structure were obtained. The resins showed excellent mechanical properties and adhesion strength. The incorporation of DGEBA contributed to crosslinking density, which can dramatically improve mechanical properties and compatibility of the coating system. The increase in the amount of polarity groups, provides a higher density of hydrogen bonds to interact with substrates. The mechanical properties and adhesion performance of the modified polysiloxane coating systems varied with epoxy contents. The marine field test in the Yellow Sea, China demonstrated that the epoxy modified polysiloxane resins possess excellent antifouling properties, demonstrating possible applications in marine anti-fouling fields.

Data availability statement

The raw/processed data required to reproduce these findings cannot be shared at this time as the data also forms part of an ongoing study.

Acknowledgements

This work was supported by National Key R&D Program of China (2016YFE0202700), National Natural Science Foundation of China (NSFC 51603053), the Application Technology Research and Development Plan of Heilongjiang Province (GX16A008), Fundamental Research Funds of the Central University, International Science & Technology Cooperation Program of China (2015DFA50050) and Defense Industrial Technology Development Program (JCKY2016604C006, JCKY2018604C011).

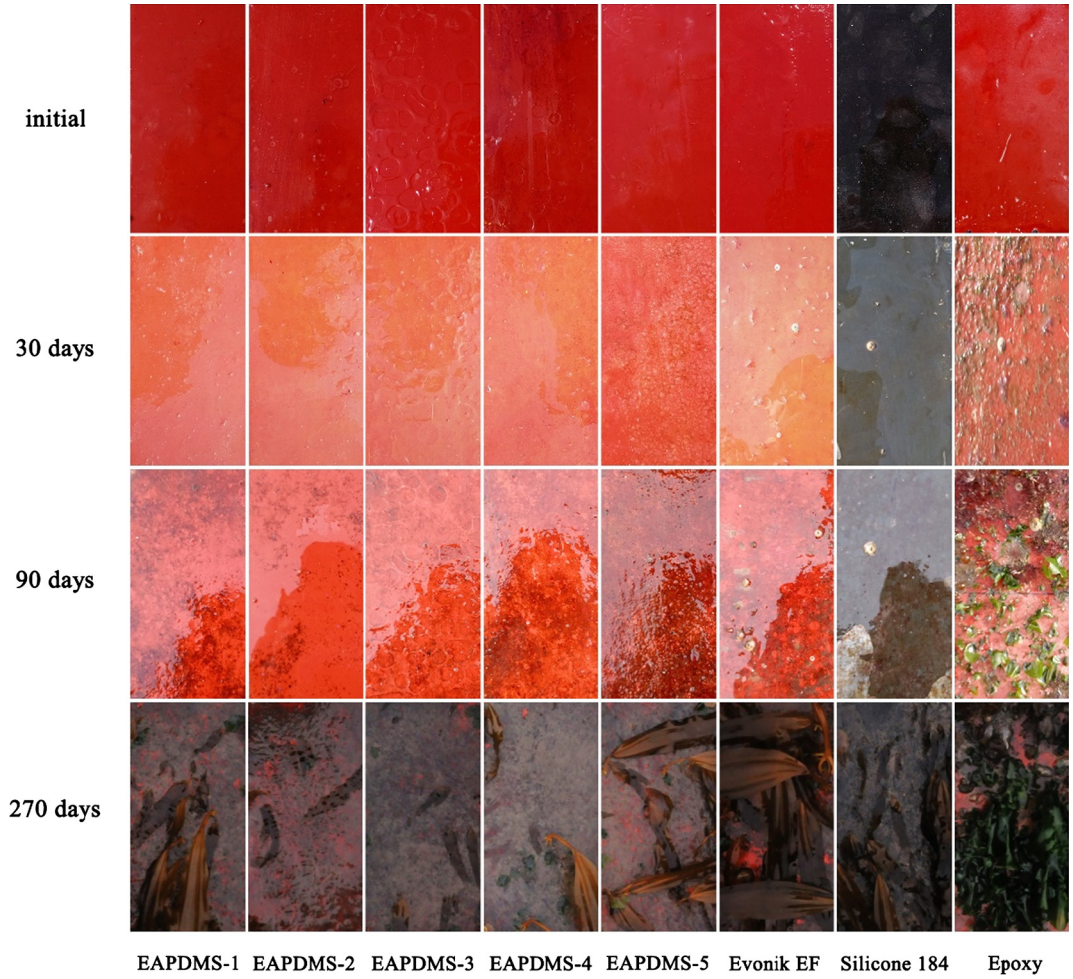

Fig. 8. Photos of EAPDMS-x, Evonik EF, Silicone 184 and pure epoxy resin coated panels after immersing in Yellow Sea, China for 30 days and 90 days. The Silicone 184 coated panel applied a black prime (XK-853, Harbin Xinke Nano Science & Technology Develop. Co. Ltd.), while other coated panels applied a red prime (D600, Qingdao Advanced Marine Material Technology Co., Ltd.).

Appendix A. Supplementary material

Supplementary data to this article can be found online at https://doi.org/10.1016/j.eurpolymj.2019.05.002.

References

[1] I. Banerjee, R.C. Pangule, R.S. Kane, Antifouling coatings: recent developments in the design of surfaces that prevent fouling by proteins, bacteria, and marine organisms, Adv. Mater. 23 (2011) 690–718.
[2] D.M. Yebra, S. Kiil, K. Dam-Johansen, Antifouling technology-past, present and future steps towards efficient and environmentally friendly antifouling coatings, Prog. Org. Coat. 50 (2004) 75–104.
[3] S. Krishnan, C.J. Weinman, C.K. Ober, Advances in polymers for anti-biofouling surfaces, J. Mater. Chem. 18 (2008) 3405–3413.
[4] J. Genzer, K. Efimenko, Recent developments in superhydrophobic surfaces and their relevance to marine fouling: a review, Biofouling 22 (2006) 339–360.
[5] B. Antizar-Ladislao, Environmental levels, toxicity and human exposure to tributyltin (TBT)-contaminated marine environment: a review, Environ. Int. 34 (2008) 292–308.
[6] P. Wang, D. Zhang, Z. Lu, Slippery liquid-infused porous surface bio-inspired by pitcher plant for marine anti-biofouling application, Colloids Surf. B-Biointerfaces 136 (2015) 240–247.
[7] U. Manna, N. Raman, M.A. Welsh, Y.M. Zayas-Gonzalez, H.E. Blackwell, S.P. Palecek, D.M. Lynn, Slippery liquid-infused porous surfaces that prevent microbial surface fouling and kill non-adherent pathogens in surrounding media: A controlled release approach, Adv. Funct. Mater. 26 (2016) 3599–3611.
[8] R. Chen, Y. Li, L. Tang, H. Yang, Z. Lu, J. Wang, L. Liu, K. Takahashi, Synthesis of zinc-based acrylate copolymers and their marine antifouling application, Rsc Adv. 7 (2017) 40020–40027.
[9] R. Chen, Y. Li, M. Yan, X. Sun, H. Han, J. Li, J. Wang, L. Liu, K. Takahashi, Synthesis of hybrid zinc/silyl acrylate copolymers and their surface properties in the microfouling stage, Rsc Adv. 6 (2016) 13858–13866.
[10] J.A. Callow, M.E. Callow, Trends in the development of environmentally friendly fouling-resistant marine coatings, Nat. Commun. 2 (2011).
[11] C.S. Gudipati, J.A. Callow, M.E. Callow, K.L. Wooley, The antifouling and fouling-release perfomance of hyperbranched fluoropolymer (HBFP)-poly(ethylene glycol) (PEG) composite coatings evaluated by adsorption of biomacromolecules and the green fouling alga Ulva, Langmuir 21 (2005) 3044–3053.
[12] R. Yang, H. Jang, R. Stocker, K.K. Gleason, Synergistic prevention of biofouling in seawater desalination by zwitterionic surfaces and low-level chlorination, Adv. Mater. 26 (2014) 1711–1718.
[13] W.J. Yang, K.-G. Neoh, E.-T. Kang, Teo, S.L.M. Teo, D. Rittschof, Polymer brush coatings for combating marine biofouling, Prog. Polym. Sci. 39 (2014) 1017–1042.
[14] T. Fyrner, H.-H. Lee, A. Lee, T. Mangone, M.E. Ekblad, M.E. Pettitt, J.A. Callow, S.L. Callow, R. Conlan, A.S. Mutton, P. Clare, B. Konradsson, T. Liedberg, Ederth, Saccharide-functionalized alkanethiols for fouling-resistant self-assembled monolayers: synthesis, monolayer properties, and antifouling behavior, Langmuir 27 (2011) 15034–15047.
[15] Y. Song, M. Liu, L. Zhang, C. Mu, X. Hu, Mechanistic interpretation of the curing kinetics of tetra-functional cyclosiloxanes, Chem. Eng. J. 328 (2017) 274–279.
[16] Y. Song, X. Tang, Y. Liang, H.Y. Lee, M. Liu, L. Zhang, S. Bi, C. Mu, X. Hu, Bioinspired reinforcement of cyclosiloxane hybrid polymer, Chem. Commun. (Cambridge, England) 54 (2018) 13415–13418.
[17] X. Zhao, Y. Su, Y. Li, R. Zhang, J. Zhao, Z. Jiang, Engineering amphiphilic membrane surfaces based on PEO and PDMS segments for improved antifouling performances, J. Membr. Sci. 450 (2014) 111–123.
[18] C. Liu, C. Ma, Q. Xie, G. Zhang, Self-repairing silicone coatings for marine antibiofouling, J. Mater. Chem. A 5 (2017) 15855–15861.
[19] C. Liu, Q. Xie, C. Ma, G. Zhang, Fouling release property of polydimethylsiloxane-based polyurea with improved adhesion to substrate, Ind. Eng. Chem. Res. 55 (2016) 6671–6676.
[20] X. Wu, J. Li, G. Li, L. Ling, G. Zhang, R. Sun, C.-P. Wong, Heat-triggered poly(siloxane-urethane)s based on disulfide bonds for self-healing application, J. Appl. Polym. Sci. 135 (2018).
[21] Z.-P. Zhang, X.-F. Song, L.-Y. Cui, Y.-H. Qi, Synthesis of polydimethylsiloxane-

modified polyurethane and the structure and properties of its antifouling coatings, Coatings 8 (2018).
[22] U. Eduok, O. Faye, J. Szpunar, Recent developments and applications of protective silicone coatings: a review of PDMS functional materials, Prog. Org. Coat. 111 (2017) 124–163.
[23] M. Esfandeh, S.M. Mirabedini, S. Pazokifard, M. Tari, Study of silicone coating adhesion to an epoxy undercoat using silane compounds-effect of silane type and application method, Colloids Surf. A-Physicochem. Eng. Aspects 302 (2007) 11–16.
[24] S.A. Kumar, T. Balakrishnan, A. Alagar, Z. Denchev, Development and characterization of silicone/phosphorus modified epoxy materials and their application as anticorrosion and antifouling coatings, Prog. Org. Coat. 55 (2006) 207–217.
[25] S.K. Rath, J.G. Chavan, S. Sasane, Jagannath, M. Patri, A.B. Samui, B.C. Chakraborty, Two component silicone modified epoxy foul release coatings: effect of modulus, surface energy and surface restructuring on pseudobarnacle and macrofouling behavior, Appl Surf Sci 256 (2010) 2440–2446.
[26] X. Ji, H. Wang, X. Ma, C. Hou, G. Ma, Progress in polydimethylsiloxane-modified waterborne polyurethanes, Rsc Adv. 7 (2017) 34086–34095.
[27] Y. Yu, J. Wang, J. Zong, Synthesis of alpha, omega-hydroxyalkyl telechelic polydimethylsiloxane soft segments and preparation of waterborne polyurethane-polydimethylsiloxane block copolymers, J. Adhes. Sci. Technol. 29 (2015) 861–874.
[28] A. Afzal, H.M. Siddiqi, A comprehensive study of the bicontinuous epoxy-silica hybrid polymers: I. synthesis, characterization and glass transition, Polymer 52 (2011) 1345–1355.
[29] F. Lionetto, M. Frigione, Environmental effects on the adhesion properties of nanostructured epoxy-silica hybrids, J. Appl. Polym. Sci. 132 (2015).
[30] X. Xia, G. Wang, P. Yang, H. Kagawa, H. Wang, M. Suzuki, W. Zhong, Q. Du, Preparation of heat-resistant epoxy/silica hybrids through a novel sol-gel process, Polym. Polym. Compos. 18 (2010) 443–450.
[31] P. Murias, H. Maciejewski, H. Galina, Epoxy resins modified with reactive low molecular weight siloxanes, Eur. Polym. J. 48 (2012) 769–773.
[32] J. Wan, S. Wang, C. Li, D. Zhou, J. Chen, Z. Liu, L. Yu, H. Fan, B. Li, Effect of molecular weight and molecular weight distribution on cure reaction of novolac with hexamethylenetetramine and properties of related composites, Thermochim. Acta 530 (2012) 32–41.
[33] L. Zhang, Y.C. Wang, X.F. Cai, Effect of a novel polysiloxane-containing nitrogen on the thermal stability and flame retardancy of epoxy resins, J. Therm. Anal. Calorim. 124 (2016) 791–798.
[34] D. Yuan, H. Yin, X. Cai, Effect of a novel flame retardant containing silicon and nitrogen on the thermal stability and flame retardancy of polycarbonate, J. Therm. Anal. Calorim. 111 (2013) 1531–1537.
[35] D. Yuan, H. Yin, X. Cai, Synergistic effects between silicon-containing flame retardant and potassium-4-(phenylsulfonyl) benzenesulfonate (KSS) on flame retardancy and thermal degradation of PC, J. Therm. Anal. Calorim. 114 (2013) 19–25.
[36] Y. Lei, G. Zheng, Y. Sun, Y. Zhou, Study on preparation and factors of amino silicone with low viscosity, Equipment Manufacturing Technology and Automation, Pts 1-3, X. Chen, Editor. 2011. pp. 2449–2453.
[37] A. Kandelbauer, G. Wuzella, A. Mahendran, I. Taudes, P. Widsten, Model-free kinetic analysis of melamine-formaldehyde resin cure, Chem. Eng. J. 152 (2009) 556–565.
[38] J. Wan, Z. Bu, C. Xu, H. Fan, B. Li, Model-fitting and model-free nonisothermal curing kinetics of epoxy resin with a low-volatile five-armed starlike aliphatic polyamine, Thermochim. Acta 525 (2011) 31–39.
[39] C. Li, C. Zuo, H. Fan, M. Yu, B. Li, Novel silicone aliphatic amine curing agent for epoxy resin: 1,3-Bis(2-aminoethylaminomethyl) tetramethyldisiloxane. 1. Non-isothermal cure and thermal decomposition property, Thermochim. Acta 545 (2012) 75–81.
[40] J. Kim, T.J. Moon, J.R. Howell, Cure kinetic model, heat of reaction, and glass transition temperature of AS4/3501-6 graphite-epoxy prepregs, J. Compos. Mater. 36 (2002) 2479–2498.
[41] R.J. Morgan, J.E. O'Neal, D.L. Fanter, The effect of moisture on the physical and mechanical integrity of epoxies, J. Mater. Sci. 15 (1980) 751–764.
[42] B. Poaty, V. Vardanyan, L. Wilczak, G. Chauve, B. Riedl, Modification of cellulose nanocrystals as reinforcement derivatives for wood coatings, Prog. Org. Coat. 77 (2014) 813–820.
[43] X. Fernández-Francos, A.O. Konuray, A. Belmonte, S.D.L. Flor, A. Serra, X. Ramis, Sequential curing of off-stoichiometric thiol-epoxy thermosets with a custom-tailored structure, Polym. Chem. 7 (2016) 2280–2290.
[44] J.M. Morancho, X. Ramis, X. Fernández-Francos, J.M. Salla, À. Serra, Curing of off-stoichiometric amine-epoxy thermosets, J. Therm. Anal. Calorim. 133 (2018) 519–527.
[45] T. He, D. Janczewski, S. Jana, A. Parthiban, S. Guo, X. Zhu, S.S.C. Lee, F.J. Parra-Velandia, S.L.M. Teo, G.J. Vancso, Efficient and robust coatings using poly(2-methyl-2-oxazoline) and its copolymers for marine and bacterial fouling prevention, J. Polym. Sci. Part A-Polym. Chem. 54 (2016) 275–283.
[46] X. Zhu, D. Janczewski, S. Guo, S.S.C. Lee, F.J.P. Velandia, S.L.M. Teo, T. He, S.R. Puniredd, G.J. Vancso, Polyion multi layers with precise surface charge control for antifouling, ACS Appl. Mater. Interfaces 7 (2015) 852–861.
[47] L.C. Paslay, B.A. Abel, T.D. Brown, V. Koul, V. Choudhary, C.L. McCormick, S.E. Morgan, Antimicrobial poly(methacrylamide) derivatives prepared via aqueous RAFT polymerization exhibit biocidal efficiency dependent upon cation structure, Biomacromolecules 13 (2012) 2472–2482.
[48] S. Sommer, A. Ekin, D.C. Webster, S.J. Stafslien, J. Daniels, L.J. VanderWal, S.E.M. Thompson, M.E. Callow, J.A. Callow, A preliminary study on the properties and fouling-release performance of siloxane-polyurethane coatings prepared from poly(dimethylsiloxane) (PDMS) macromers, Biofouling 26 (2010) 961–972.
[49] R. Holland, T.M. Dugdale, R. Wetherbee, A.B. Brennan, J.A. Finlay, J.A. Callow, M.E. Callow, Adhesion and motility of fouling diatoms on a silicone elastomer, Biofouling 20 (2004) 323–329.
[50] L. Hoipkemeier-Wilson, J. Schumacher, M. Carman, A. Gibson, A. Feinberg, M. Callow, J. Finlay, J. Callow, A. Brennan, Antifouling potential of lubricious, micro-engineered, PDMS elastomers against zoospores of the green fouling alga Ulva (Enteromorpha), Biofouling 20 (2004) 53–63.
[51] S. Venkataraman, Y. Zhang, L. Liu, Y.-Y. Yang, Design, syntheses and evaluation of hemocompatible pegylated-antimicrobial polymers with well-controlled molecular structures, Biomaterials 31 (2010) 1751–1756.
[52] K. Kuroda, W.F. DeGrado, Amphiphilic polymethacrylate derivatives as antimicrobial agents, J. Am. Chem. Soc. 127 (2005) 4128–4129.
[53] E.F. Palermo, K. Kuroda, Chemical structure of cationic groups in amphiphilic polymethacrylates modulates the antimicrobial and hemolytic activities, Biomacromolecules 10 (2009) 1416–1428.
[54] E.F. Palermo, I. Sovadinova, K. Kuroda, Structural determinants of antimicrobial activity and biocompatibility in membrane-disrupting methacrylamide random Copolymers, Biomacromolecules 10 (2009) 3098–3107.